Modeling COVID-19: Forecasting and analyzing the dynamics of the outbreaks in Hubei and Turkey

IBRAHIM HALIL ASLAN

Department of Mathematics, Batman University, West Ramada
Batman, 72000, Turkey
ibrahimhalil.aslan@batman.edu.tr

MAHIR DEMIR

Department of Fisheries and Wildlife/Quantitative Fishery Center, Michigan State University
East Lansing, 48823, MI, USA
demirmah@msu.edu

MICHAEL MORGAN WISE

Department of Mathematics, University of Tennessee at Knoxville
Knoxville, 37996, TN, USA
mwise9@vols.utk.edu

SUZANNE LENHART

Department of Mathematics, University of Tennessee at Knoxville
Knoxville, 37996, TN, USA
lenhart@math.utk.edu

April 13, 2020

Abstract

As the pandemic of Coronavirus Disease 2019 (COVID-19) rages worldwide, accurate modeling of the dynamics thereof is essential. However, since the availability and quality of data varies dramatically from region to region, accurate modeling directly from a global perspective is difficult, if not altogether impossible. Nevertheless, via local data collected by certain regions, it is possible to develop accurate local prediction tools, which may be coupled to develop global models.

In this study, we analyze the dynamics of local outbreaks of COVID-19 via a coupled system of ordinary differential equations (ODEs). Utilizing the large amount of data available from the ebbing outbreak in Hubei, China as a testbed, we estimate the basic reproduction number $\mathcal{R}_0$ of COVID-19 and predict the total cases, total deaths, and other features of the Hubei outbreak with a high level of accuracy. Through numerical experiments, we observe the effects of quarantine, social distancing, and COVID-19 testing on the dynamics of the outbreak. Using knowledge gleaned from the Hubei outbreak, we apply our model to analyze the dynamics of outbreak in Turkey. We provide forecasts for the peak of the outbreak and the total number of cases/deaths in Turkey, for varying levels of social distancing, quarantine, and COVID-19 testing.

Keywords: quarantine, social distancing, COVID-19 testing, novel coronavirus, COVID-19, reproduction number, forecasting, ordinary differential equations.

1 Introduction

In late 2019, the city of Wuhan in the province of Hubei, China experienced an outbreak of Coronavirus Disease 2019 (COVID-19), the disease caused by the novel coronavirus SARS Coronavirus 2 (SARS-CoV-2). This outbreak quickly spread to all states of China and across the globe, being declared a pandemic by the World Health Organization (WHO) on 11 March 2020. The authorities imposed a strict lockdown on the city of Wuhan and the rest of the Hubei province in late January 2020, [1]. In the face of over sixty-seven thousand cases and over three thousand deaths, the authorities continued strict enforcement of these measures [2, 3]. Finally, on 23 March 2020, Hubei reached a significant milestone as the province's health commission reported no new cases for seven consecutive days [1, 4]. Shortly thereafter, after over two months of severe restrictions on the movements of the Hubei population, the "2020 Hubei Lockdowns" were relaxed as the Hubei outbreak began to wane, inspiring hope that the pandemic ravaging the globe might be able to be controlled via quarantine and social distancing measures.

Previous studies of COVID-19 provided the evidence of human-to-human transmission and revealed its similarity and differences from SARS [5, 6, 7]. However, data-driven simulation-based studies are needed to understand the dynamics of the ongoing outbreak. Indeed, it is of the utmost importance to use these tools to investigate the effectiveness of public health strategies, such as the number of COVID-19 tests carried out to detect the infected, the level of quarantine/social distancing, and its efficiency in the transmission of COVID-19. Many (preprint) studies investigate dynamics of this pandemic from a global perspective (see, e.g., [8, 9, 10, 11, 12, 13]. Nevertheless, the large variations in both quality and availability of data from region to region make direct global modeling of the dynamics of this pandemic exceedingly difficult.

As a result, in this study, we develop a model for dynamics of the pandemic from a local perspective. The numerous "hotspots" of COVID-19 combined with the restrictions on travel in place throughout the world further suggest that local models might provide better insight into the dynamics than their global counterparts. Also, accurate models for local regions can be coupled to develop reasonable models for larger regions.

As of 23 March 2020, around one-quarter of the global COVID-19 cases and consequent deaths occurred in Hubei. The large proportion of data available from Hubei combined with the region's recent achievements toward managing their local outbreak suggest that the data from this region presents an excellent picture of the lifetime of an outbreak of COVID-19. Indeed, as countries worldwide close their borders, cities and regions, and impose their own "shelter-in-place," quarantine, or lockdown orders in the face of the pandemic, the large amount of data available from Hubei provides an excellent testbed for modeling the dynamics of a local outbreak of COVID-19.

In this study, we start by developing a SEIQR type deterministic model which employs a system of ordinary differential equations to analyze the dynamics of the local outbreak, highlighting the effect of testing and the effects of quarantine and social distancing in Hubei. We present estimates of the basic reproductive number $\mathcal{R}_0$ of COVID-19 in Hubei and perform a sensitivity analysis to deduce which parameters play significant roles in the transmission and control of the outbreak in Hubei. In addition, we also provide 15-day forecasts of the fatality rate of the outbreak, the number of cases, and the number of deaths depending on the data [2, 3, 1] and outputs of our SEIQR model. Finally, building on knowledge obtained from the Hubei outbreak, we apply our model to the outbreak in Turkey. We forecast the peak of the outbreak and the total number of cases/deaths in Turkey, utilizing the extant COVID-19 data from Turkey [14].

2 Model formulation

In this section, we develop a deterministic compartmental model using ordinary differential equations (ODEs) to understand the dynamics of COVID-19 in Hubei, China [15, 16, 17]. In the model, the total population $N(t)$ at time t (in days) is divided into the following six compartments: susceptible $S(t)$, susceptible in quarantine (isolated class) $S_q(t)$, exposed $E(t)$, infected (asymptomatic or having mild symptoms) $I(t)$, reported (infected) cases (hospitalized if get severe symptoms or quarantined if get mild symptoms) $I_q(t)$, and recovered $R(t)$. Note that all individuals who, upon testing, test positive are immediately isolated. Figure 1 shows the transition flows among the compartments of

the model. The rate of reported cases i_q denotes the number of individuals who transition from the infected class I to the reported class I_q per day; it is also directly related to the daily number of COVID-19 tests carried out during the outbreak. Also, note that the reduction rate r is associated with the efficiency of quarantine, such as social distancing and wearing medical masks.

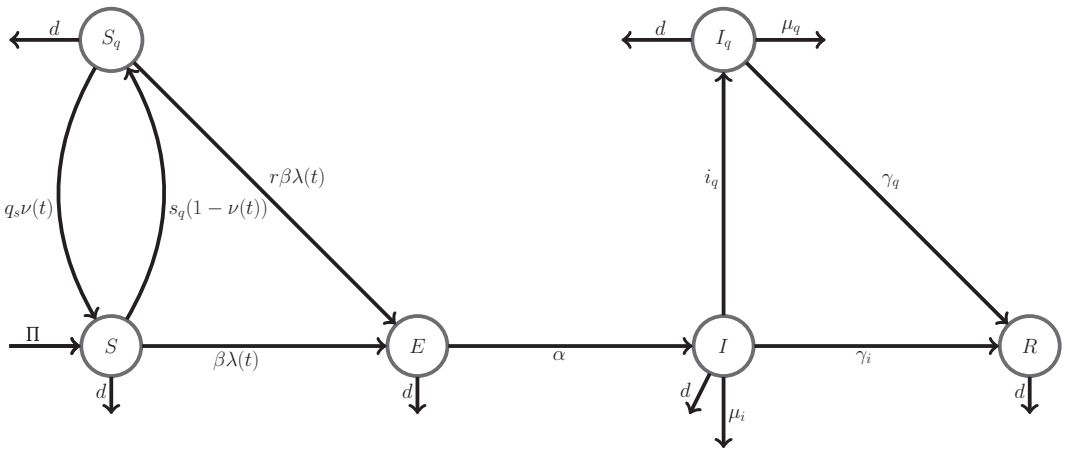

Figure 1: Flow diagram illustrating the disease transitions among the compartments

Susceptible individuals transition to the $S_q(t)$ compartment with a rate of

$$s_q(1-\nu(t))S$$

where $\nu(t) = e^{-I_q(t)}$. Note that the main indicator of quarantine is the number of reported cases I_q. When the number of reported cases increases in a state or country, then the quarantine is imposed or naturally taken as an option. Thus, when the number of reported cases increases, then percentage or amount of people quarantined will increase. If the number of reported cases falls to zero, the transition rate from S to S_q is zero and from S_q to S is q_s. The individuals in S and S_q compartments transition to compartment E (exposed) with a force of infection given by

$$\lambda(t) = \frac{I(t)}{N(t)}$$

and disease transmission rate β. Note that, since the individuals in S_q transition to E compartment less frequently, a reduction factor r is taken into count in the model. After an incubation period of $1/\alpha$, the individuals in E compartment transition to I compartment (infected) with rate α. The individuals in I compartment will transition to either R compartment (recovered) with a rate of γ_i, I_q compartment with a rate of i_q, or die due to the disease with a rate of μ_i. The individuals in I_q (reported (infected) individuals who are hospitalized or quarantined) compartment either transition to R compartment with a rate of γ_q or die due to disease with a rate of μ_q. The following (ODEs) system represents the dynamical behavior of the system.

$$
\begin{aligned}
\frac{dS(t)}{dt} &= \Pi + q_s e^{-I_q(t)} S_q(t) - s_q(1 - e^{-I_q(t)})S(t) - \beta\lambda(t)S(t) - dS(t) \\
\frac{dS_q(t)}{dt} &= s_q(1 - e^{-I_q(t)})S(t) - q_s e^{-I_q(t)} S_q(t) - r\beta\lambda(t)S_q(t) - dS_q(t) \\
\frac{dE(t)}{dt} &= \beta\lambda(t)S(t) + r\beta\lambda(t)S_q(t) - \alpha E(t) - dE(t) \\
\frac{dI(t)}{dt} &= \alpha E(t) - i_q I(t) - \gamma_i I(t) - \mu_i I(t) - dI(t) \\
\frac{dI_q(t)}{dt} &= i_q I(t) - \gamma_q I_q(t) - \mu_q I_q(t) - dI_q(t) \\
\frac{dR(t)}{dt} &= \gamma_i I(t) + \gamma_q I_q(t) - dR(t)
\end{aligned} \tag{1}
$$

with $S(0) > 0, S_q(0) \geq 0, E(0) \geq 0, I(0) \geq 0, I_q(0) \geq 0, R(0) \geq 0$ and $N(t) = S(t) + S_q(t) + E(t) + I(t) + I_q(t) + R(t)$

The left hand side of the system (1) represents the rate of change of each compartment. In the system (1), we have

$$
\begin{aligned}
\frac{d}{dt}(S + S_q + E + I + I_q + R) &= \Pi - d(S + S_q + E + I + I_q + R) - \mu_i I - \mu_q I_q \\
&\leq \Pi - d(S + S_q + E + I + I_q + R) \\
&\Rightarrow \limsup_{t \longrightarrow \infty}(S + S_q + E + I + I_q + R) \leq \frac{\Pi}{d}
\end{aligned}
$$

Hence, the feasible region of the system (1) is given by

$$
\Gamma = \left\{ (S, S_q, E, I, I_q, R) : (S + S_q + E + I + I_q + R) \leq \frac{\Pi}{d}, S(0) > 0, S_q(0) \geq 0, E(0) \geq 0, I(0) \geq 0, I_q(0) \geq 0, R(0) \geq 0 \right\}
$$

This implies all the compartments remain non-negative. The parameter values used in the model are given in Table 1 with their description and units.

Table 1: Parameter descriptions and values

Parameter	Description	Value	Unit	Source
$\mathcal{R}_0$	The basic reproduction number	5.49	-	Estimated
β	Disease transmission rate	5.24	$\frac{1}{\text{day}}$	Estimated
q_s	Rate of release from quarantine	0.5	$\frac{1}{\text{day}}$	Estimated
s_q	Quarantine rate of susceptible individuals	0.096	$\frac{1}{\text{day}}$	Estimated
α	Rate of exposed individuals becoming infected	0.2381	$\frac{1}{\text{day}}$	[18, 19, 20]
γ_i	Recovery rate due to natural immune response	0.111	-	Estimated
γ_q	Recovery rate due to hospitalization	0.107	$\frac{1}{\text{day}}$	Estimated
μ_i	Death rate of disease in infectious compartment	0.0096	$\frac{1}{\text{day}}$	Estimated
μ_q	Death rate due to disease in reported infectious compartment	0.004	$\frac{1}{\text{day}}$	Estimated
i_q	Rate of reported (infected) individuals	0.832	$\frac{1}{\text{day}}$	Estimated
r	Reduction rate in transmission due to quarantine	0.011	-	Estimated
Π	Recruitment rate	2134	$\frac{\text{Individual}}{\text{day}}$	[21]
d	Natural death rate	0.000023	$\frac{1}{\text{day}}$	[21]
$E(0)$	Initial number of exposed Individuals	142	Individual	Estimated
$I(0)$	Initial number of infected Individuals	69	Individual	Estimated

3 Diseases free equilibrium and stability analysis

One of major concepts in an outbreak is disease free equilibrium (DFE), where the entire population is susceptible [16, 22]. For the system (1), the DFE can be denoted

$$x^* = (S^*, S_q^*, E^*, I^*, I_q^*, R^*) = (S^*, 0, 0, 0, 0, 0).$$

To obtain the DFE for the system (1), we set the right hand side of the system (1) to zero and substitute the DFE into the system. Hence, the DFE is given by

$$x^* = (S^*, S_q^*, E^*, I^*, I_q^*, R^*) = (\frac{\Pi}{d}, 0, 0, 0, 0, 0).$$

For stability analysis of the DFE, we employ the next-generation matrix (NGM) [23, 22, 24]. We rewrite our system (1) as:

$$x_i' = f_i(x) = \mathscr{F}_i(x) - \mathscr{V}(x) = \mathscr{F}_i(x) - (\mathscr{V}_i^-(x) - \mathscr{V}_i^+(x))$$

where $x = (S^*, S_q^*, E^*, I^*, I_q^*, R^*)$ and $i = 1, 2, \ldots, 6$ and

- $\mathscr{F}_i(x)$:= Rate of appearance of new infections in compartment i
- $\mathscr{V}_i^+(x)$:=Rate of transfer of individuals into compartment i by all other means
- $\mathscr{V}_i^-(x)$:= Rate of transfer of individuals out of compartment i by all other means.

Hence, $\mathscr{F}$ and $\mathscr{V}$ are calculated for the system of (1):

$$\mathscr{F} = \begin{bmatrix} \beta\lambda(t)S(t) + r\beta\lambda(t)S_q(t) \\ 0 \\ 0 \\ 0 \\ 0 \\ 0 \end{bmatrix}$$

and

$$\mathscr{V} = \begin{bmatrix} \alpha E(t) + dE(t) \\ -\alpha E(t) + i_q I(t) + \gamma_i I(t) + \mu_i I(t) + dI(t) \\ -i_q I(t) + \gamma_q I_q(t) + \mu_q I_q(t) + dI_q(t) \\ -\Pi - q_s e^{-I_q(t)} S_q(t) + s_q(1 - e^{-I_q(t)})S(t) + \beta\lambda(t)S(t) + dS(t) \\ -s_q(1 - e^{-I_q(t)})S(t) + q_s e^{-I_q(t)} S_q(t) + r\beta\lambda(t)S_q(t) + dS_q(t) \\ -\gamma_i I(t) - \gamma_q I_q(t) + dR(t) \end{bmatrix}$$

Notice that individuals which transition to E compartment are the only newly infected cases. Therefore, the Jacobian at the DFE for the infected classes (first three components, x) are

$$\mathbf{F}(\mathbf{X}^*) = \begin{bmatrix} 0 & \beta & 0 \\ 0 & 0 & 0 \\ 0 & 0 & 0 \end{bmatrix}$$

and

$$\mathbf{V}(\mathbf{X}^*) = \begin{bmatrix} \alpha + d & 0 & 0 \\ -\alpha & i_q + \gamma_i + \mu_i + d & 0 \\ 0 & -i_q & \gamma_q + \mu_q + d \end{bmatrix}$$

We compute the next generation matrix (NGM) as

$$\mathbf{F}(\mathbf{X}^*)\mathbf{V}(\mathbf{X}^*)^{-1} = \begin{bmatrix} \frac{\alpha\beta}{(\alpha+d)(i_q+\gamma_i+\mu_i+d)} & \frac{\beta}{i_q+\gamma_i+\mu_i+d} & 0 \\ 0 & 0 & 0 \\ 0 & 0 & 0 \end{bmatrix} \tag{2}$$

The spectral radius of the NGM is the basic reproduction number $\mathcal{R}_0$ defined to be the average number of secondary cases arising from an average primary infected case in an entirely susceptible population. The DFE is locally stable if $\mathcal{R}_0 < 1$ [23, 22]. The spectral radius of the NGM given in (2)

$$\rho(\mathbf{F}\mathbf{V}^{-1}) = \mathcal{R}_0 = \frac{\alpha\beta}{(\alpha + d)(i_q + \gamma_i + \mu_i + d)}$$

Since we do not consider the individuals in S_q compartment as a part of the DFE, we quarantine does not affect the value of $\mathcal{R}_0$ directly. However, s_q indirectly changes the other parameter values such as β and i_q so that $\mathcal{R}_0$ indeed varies with s_q, albeit indirectly. Note that α and β are positively correlated with $\mathcal{R}_0$ and i_q, γ_i, μ_i and d are negatively correlated with $\mathcal{R}_0$ for the system (1). Note that we might control the disease with increasing quarantine rate of infected individual i_q. Indeed, if

$$i_q > \frac{\alpha\beta}{(\alpha + d)} - \gamma_i - \mu_i - d$$

then the DFE is locally stable and the disease dies out when sufficiently close to DFE. Biologically, if the infected individuals can be detected and quarantined in a sufficiently short time, the disease can be controlled.

4 Parameter estimation

In this part, we estimate the parameters in the system (1) fitting our model with the available data for cumulative number of cases and deaths provided by [1] and [2]. We use the Ordinary Least Squares (OLS) method and minimize the sum of the squares of differences between the daily reported data and those predicted by our model. The goodness of the fit is measured by computing the associated relative error of the fit using the formula

$$\min \left(\frac{\sum_{i=1}^{n} (C_i - \hat{C}_l)^2}{\sum_{i=1}^{n} C_i^2} + \frac{\sum_{i=1}^{n} (D_i - \hat{D}_l)^2}{\sum_{i=1}^{n} D_i^2} \right) \approx 0.06 \tag{3}$$

where C_i and $\hat{C}_l$ are exact and estimated cumulative(infected) cases, and D_i and $\hat{D}_l$ are exact and estimated cumulative deaths. To estimate the number of COVID-19 deaths, we sum the number of deaths coming from the infected class I and the reported (infected) class I_q. Note that the natural deaths in the infected class I and the reported (infected) class I_q are also included in the total number of deaths. We used an ode45 solver with fmincon from the Optimization Toolbox of MATLAB. By using the initial conditions: $S(0) = 59,000,000$, $S_q(0) = 0$, $I_q(0) = 258$, and $R(0) = 0$, we estimate all the parameters of the model together with estimating the initial number of exposed E and infected I, except the natural death rate d, recruitment rate Π, and incubation period α. We used 4.2 days for the average incubation period, in keeping with [18, 19, 20]. The natural death and recruitment rate are provided by the WHO [21].

The simulation results obtained for the cumulative number of (infected) cases C and cumulative deaths D by fitting the model with the data from January 20, 2020 to March 23, 2020 are depicted in Figure 2. These figures show a

reasonably good fit with the total relative error 0.06 (6%). Most of the error comes from the fit of cumulative cases, especially around February 12, 2020. In February, China began to report clinically diagnosed cases in addition to laboratory-confirmed cases, and on February 12, 2020, 13,332 clinically (rather than laboratory) diagnosed cases were reported even though they were diagnosed in the preceding days and weeks. Due to the very small number of cases reported after March 23, 2020, we chose to fit the model only using data from before this date.

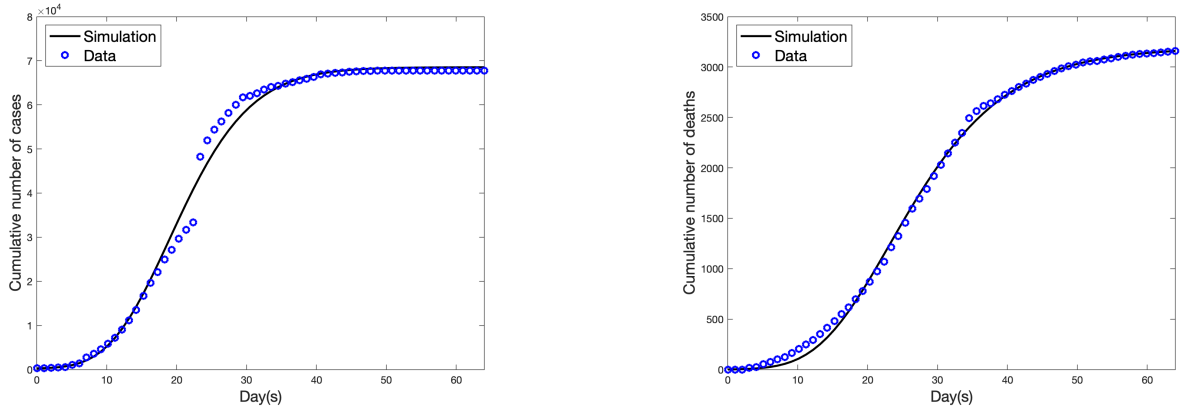

Figure 2: Fitting the model to the data from January 20, 2020 to March 23, 2020 in Hubei: the cumulative number of (infected) cases and deaths (Parameter values used are as given in Table 1).

5 Simulations

In this section, we discuss 15-day forecasts of the outbreak and the effects of quarantine and testing in Hubei. We also conduct a sensitivity analysis to elucidate which parameters play important roles in the dynamics of the outbreak.

5.1 Effect of quarantine (Self-isolation)

Nearly the entire province of Hubei was quarantined by February 15, 2020 (See Figure 3. Note that February 15 corresponds the day 25 in the figure.). The percentage of the population transitioning from the susceptible class to the quarantine class attained its maximum level between January 27, 2020 and February 10, 2020, and by February 15, almost all of the population were in quarantine. This result makes sense since the state imposed a quarantine in the province in late January, initially recommending quarantine to minimize social contact and finally forcing the population into quarantine to guarantee social distancing. This action seems to have worked to great effect, reducing the contact rate by about 98.9% (See Table 1 for the parameter r, the reduction rate for transmission due to the quarantine).

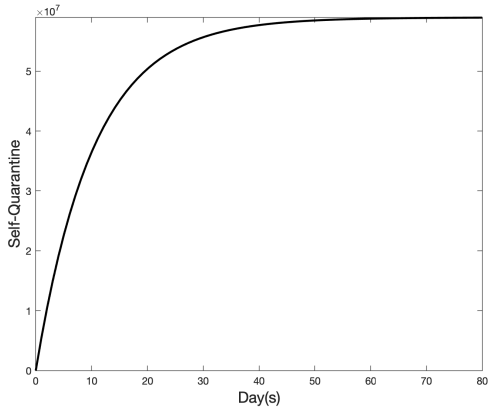

Figure 3: Transitions from the susceptible class to the quarantine class during the outbreak in Hubei

When we reduce the quarantine rate, s_q from 0.096 to 0.0864 (10% reduction) and do not change the remaining parameters, the number of cases and deaths would be about 141,090 and 6,562, respectively. Similarly, when we increase the quarantine rate, s_q from 0.096 to 0.1056 (10% increase), the number of cases and deaths would be about 39,334 and 1,829, respectively. Thus, any change in the quarantine rate makes very significant change in total number of cases and deaths. Furthermore, see the sensitivity analysis section below, the quarantine rate is a significant parameter in the dynamics of the outbreak as well as its efficiency, which is explained by the parameter, r is also significant in the dynamic of the outbreak.

5.2 15-day Forecasting

We used the parameters in Table 1 to run 15-day forecasts. Figure 4 shows the estimated number of infected cases for 80 days. The plot on the left depicts the estimated number of exposed and the right plot depicts the estimated number of reported (infected) cases I_q. As it can be seen, the number of individuals in each of these classes tends to zero, which implies that the outbreak is waning. As it can be seen from the behavior of the infected class, the outbreak reaches its peak about February 9, 2020. The infected class I, of course, also includes infected individuals who present no symptoms or mild symptoms.

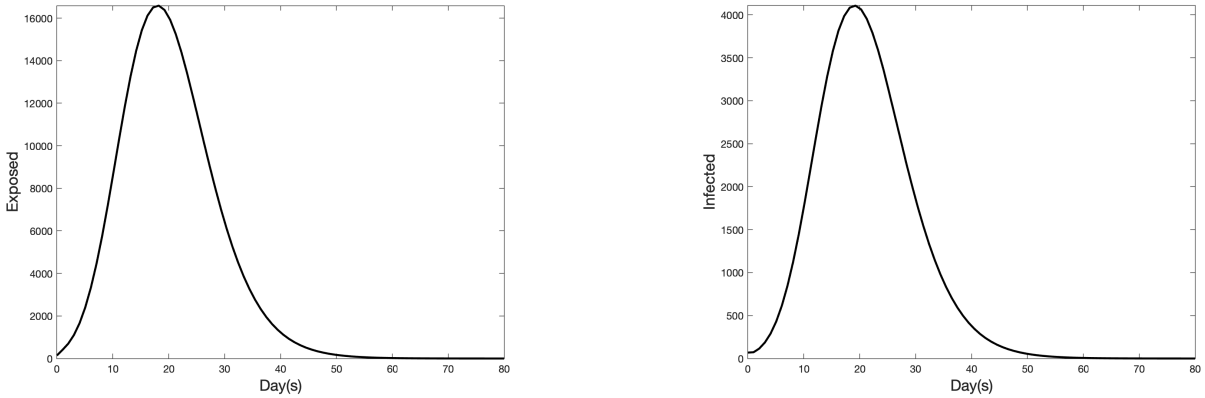

Figure 4: The plot on the left depicts the number of exposed cases and the plot on the right depicts the number of infected cases with initial conditions $S(0) = 59,000,000, S_q(0) = 0, E(0) = 142, I(0) = 69, I_q(0) = 258, R(0) = 0$ for 80 days

In Figure 5, the plot on the left shows the estimated number of reported (infected) cases accumulated and the

right plot shows the estimated total number of deaths accumulated. As of 30 March 2020, there were no reported cases in Hubei in the preceding week and the total number of cases and total number of deaths were 67,801 and 3,187, respectively. Our model (1), predicts the number of cases and deaths with high accuracy with 6 percent relative error. We estimated the fatality rate of the outbreak in Hubei as approximately 4.8% with the estimated number of cases, about 67,994 and deaths, about 3,254.

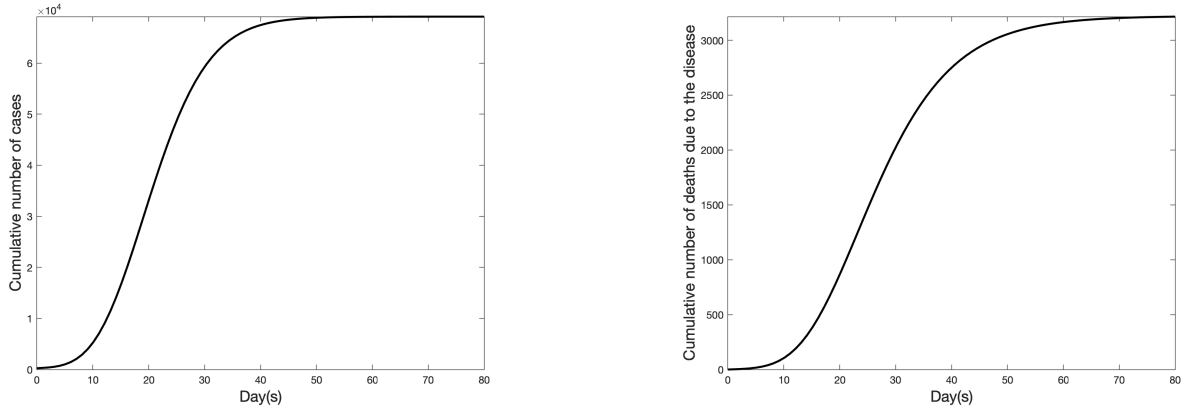

Figure 5: The plot on the left depicts the simulated cumulative number of infected cases due to the outbreak and the plot on the right depicts the simulated cumulative number of deaths in Hubei

5.3 Sensitivity analysis

Several parameters play important roles in the model (1). These parameters were estimated with existing data from [3]. In order to determine the set of parameters that are statistically significant with regard to the number of cumulative infected cases, we conduct a sensitivity analysis of the model. We utilized a Latin Hypercube Sampling (LHS) and the Partial Rank Correlation Coefficients (PRCC) method [25]. We use a range given in Table 2 to sample parameters from a uniform distribution, then use these samples as input variables when we run the system (1) for 90 days with initial conditions $S(0) = 1000, S_q(0) = 0, E(0) = 10, I(0) = 3, I_q(0) = 0, R(0) = 0$. The number of cumulative infected cases is the output variables in sensitivity analysis. Table 2 shows PRCC values, p-values and the range for each corresponding parameters.

Table 2: Results of sensitivity analysis with partial rank correlation coefficient (PRCC), p-value. The range considered for each parameter is included in the final column

Parameter	PRCC	p-value	Range
β	0.89	1.2e-104	[1, 10]
q_s	-0.084	0.15	[0.1, 0.9]
s_q	-0.45	3.4e-16	[0.01, 0.2]
α	0.23	6.9e-05	[0.05, 0.5]
γ_i	-0.25	1.3e-05	[0.01, 0.2]
γ_q	-0.075	0.2	[0.01, 0.4]
μ_i	-0.052	0.37	[0.001, 0.2]
μ_q	0.12	0.032	[0.001, 0.2]
i_q	-0.81	3.1e-70	[0.5, 4]
r	0.69	8.3e-44	[0.001, 0.9]
Π	-0.05	0.39	[0.01, 0.1]
d	0.067	0.25	[0.000001, 0.0001]

The sensitivity analysis indicates that β, s_q, i_q, and r are statistically more significant parameters due to the high PRCC values in the dynamics of the outbreak. Therefore, it is of interest to study how the number of cumulative infected

cases changes when s_q, i_q, r, and β are varied and all other parameters are held the same as in Table 1 and the initial condition is taken the same as before. Figure 6 shows the results of these experiments, namely, how the cumulative number of cases changes for different values of s_q, i_q, r, and β.

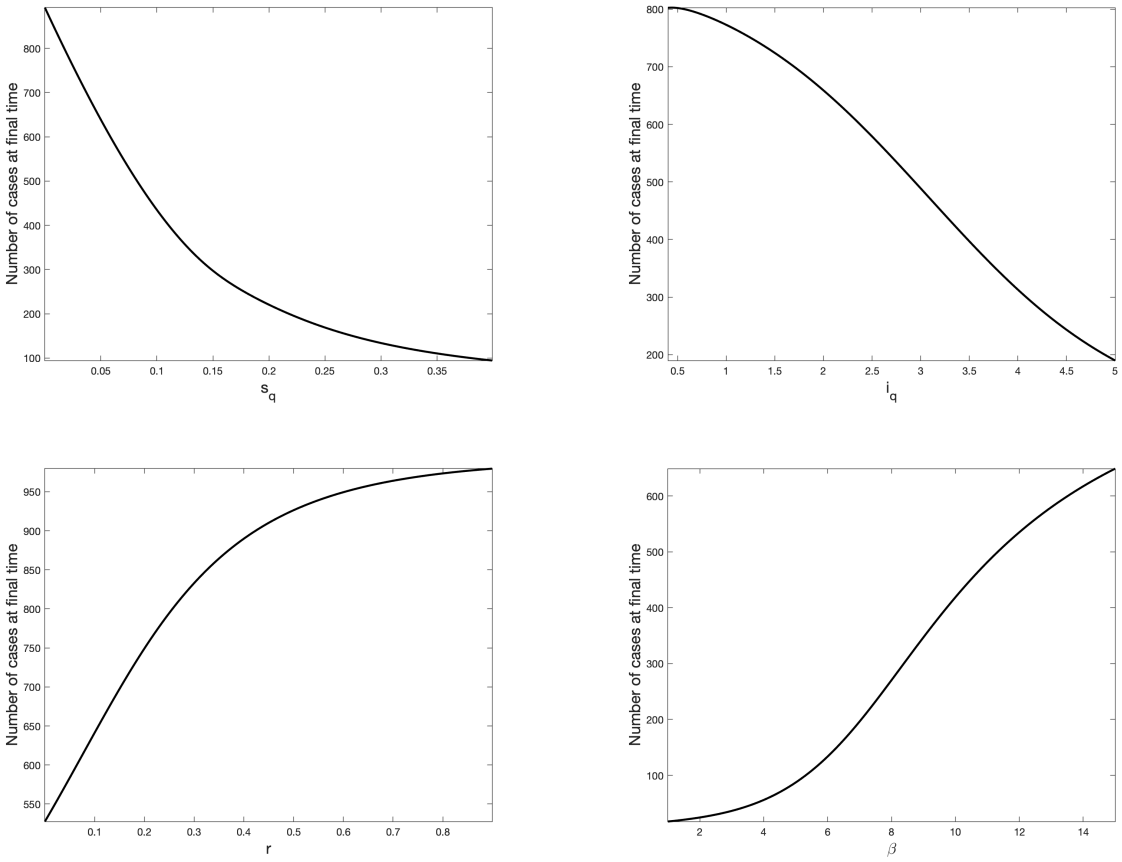

Figure 6: Number of cases at final time with respect to the transmission rate β, quarantine rate s_q, rate of reported cases i_q, and reduction rate r.

Figure 6 shows that an increase in the quarantine rate s_q sharply decreases the cumulative number of cases and that an increase in the quarantine rate of infected individuals i_q decreases the number of new cases. Increasing the reduction rate r due to the quarantine increases the cumulative number of cases and increasing the disease transmission rate, β increases the number of cases.

It is also important to analyze how $\mathcal{R}_0$ varies in relation to β and i_q. As a result, we vary β in the range $[1, 10]$ and i_q in the range $[0.1, 4]$, holding all other parameters the same as in Table 1. Figure 7 shows boxplots of β and i_q. We observe that i_q affects $\mathcal{R}_0$ in a wider range than does β. Thus, the range of $\mathcal{R}_0$ will generally remain between 3 and 8. It is of note that the value of $\mathcal{R}_0$ drops below 1 when i_q is above 5.1.

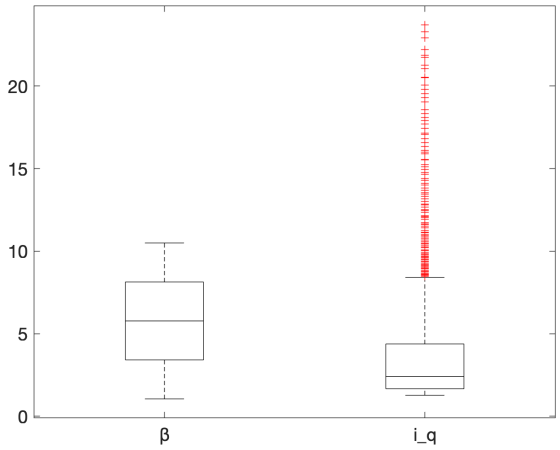

Figure 7: Change in $\mathcal{R}_0$ when we vary β with the rage [1,10], or i_q with the range [0.1, 4].

The rate of reported cases i_q is related to the number of tests given during the outbreak to identify the infected people. Thus, increasing the number of tests will increase the rate of case reporting i_q. This will reduce the number of cases (see Figure 6) and, consequently, the number of deaths due to the outbreak. When we increase the rate of reported (infected) cases i_q by about 10%, the number of cases and number of deaths are estimated to be 36,040 and 1,639, respectively. Decreasing the rate by about 10%, the number of cases and number of deaths are estimated to be 14,084 and 6,724, respectively.

6 Forecasting the peak of the outbreak, number of cases/deaths in Turkey

In this part, we fit the model (1) with available COVID-19 data from Turkey [14]. We consider data from March 10, 2020 to April 10, 2020, and achieve a fit (see equation (3)) with approximately 5.9% relative error. We estimate the four parameters i_q, s_q, β, and r, which are not only the most significant parameters in the dynamics of outbreak, but also tend to be specific to each local region. Therefore, by using the initial conditions: $S(0) = 83,000,000$, $S_q(0) = 0$, $I_q(0) = 1$, and $R(0) = 0$, we estimate these four parameters together with the initial number of exposed and infected individuals. We do not estimate the rest of the parameters, employing the parameters in Table 1. As a result, our results in this section builds upon existing knowledge regarding dynamics of a local COVID-19 outbreak gleaned from study of the Hubei outbreak in addition to the available Turkish data [14]. Note that the quarantine rate and the rate of reported cases (which, we stress, is related to number of COVID-19 tests) can be increased. Indeed, this increase still may have significant effect toward the reduction of the number of cases (See Figure 6, sensitivity analysis). However, increasing the reduction rate r will not effect significant changes in the number of cases in Turkey since r is already very close to its maximum level (See Figure 6). Thus, we will vary only the quarantine rate s_q and the rate of reported cases i_q as we forecast the peak of the outbreak and the total number of cases/deaths in Turkey.

Table 3: Parameter descriptions and values of the model (1) with Turkish data.

Parameter	Description	Value	Unit	Source
$\mathcal{R}_0$	The basic reproduction number	5.2	-	Estimated
β	Disease transmission rate	9.98	$\frac{1}{\text{day}}$	Estimated
s_q	Quarantine rate of susceptible individuals	0.088	$\frac{1}{\text{day}}$	Estimated
i_q	Rate of reported (infected) individuals	1.8	$\frac{1}{\text{day}}$	Estimated
r	Reduction rate in transmission due to quarantine	0.15	-	Estimated
Π	Recruitment rate	3827	$\frac{\text{Individual}}{\text{day}}$	[21]
d	Natural death rate	0.000016	$\frac{1}{\text{day}}$	[21]
$E(0)$	Initial number of exposed Individuals	6	Individual	Estimated
$I(0)$	Initial number of infected Individuals	2	Individual	Estimated

The rate of reported cases is about 1.8; this rate is larger than what we observed in Hubei. This implies that in terms of numbers of COVID-19 tests conducted per day, Turkey is now testing more than Hubei, China was at a comparable time in Hubei's outbreak. The efficiency of quarantine also seems to be very good in Turkey, given the approximately 85% reduction in the contact rate of COVID-19 obtained by our parameter estimation. On the other hand, the quarantine rate is about 0.088, which is small when compared with the quarantine rate in Hubei (the rate was 0.096). In Hubei, the population transitioned to quarantine class very quickly (in approximately two weeks), but in Turkey the transition to quarantine has been very slow in comparison (see Figure 8). This may provide some insight into why the contact rate is higher in Turkey when compared to the contact rate in Hubei (See Table 1 and 3 for these rates).

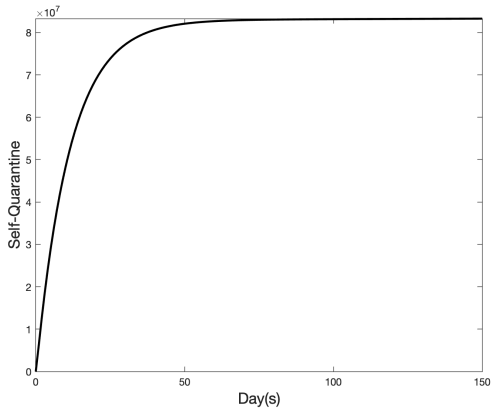

Figure 8: Transitions from the susceptible class to the quarantine class during the outbreak in Turkey after the first cases reported on March 10, 2020

It is yet possible to increase the quarantine rate (the rate of transition to quarantine class) and the number of COVID-19 tests given each day in Turkey to effect a reduction in the number of cases and deaths (See Figures 9 and 10). In Figures 9 and 10, the red curves are obtained using base parameters from Table 1 and 3, and the other curves obtained by varying the quarantine rate s_q and the rate of reported cases i_q. When we use the base parameter values which are obtained from our fitting, Turkey then will have about 203,700 cases and 8,269 deaths. If Turkey can increase the number of individuals in quarantine and the number of daily COVID-19 tests, then, depending on the magnitude of the increases, the number of cases and deaths can decrease significantly (see Figures 9 and 10). When we look at trajectories of cumulative cases and deaths in Figures 9 and 10, in the worst-case scenario (the black curves) of the study, Turkey will have about 281,500 cases and 11,430 deaths. These projections decrease to 148,100 cases and 6,005 deaths if Turkey can increase the number of individuals in quarantine and the number of COVID-19 tests.

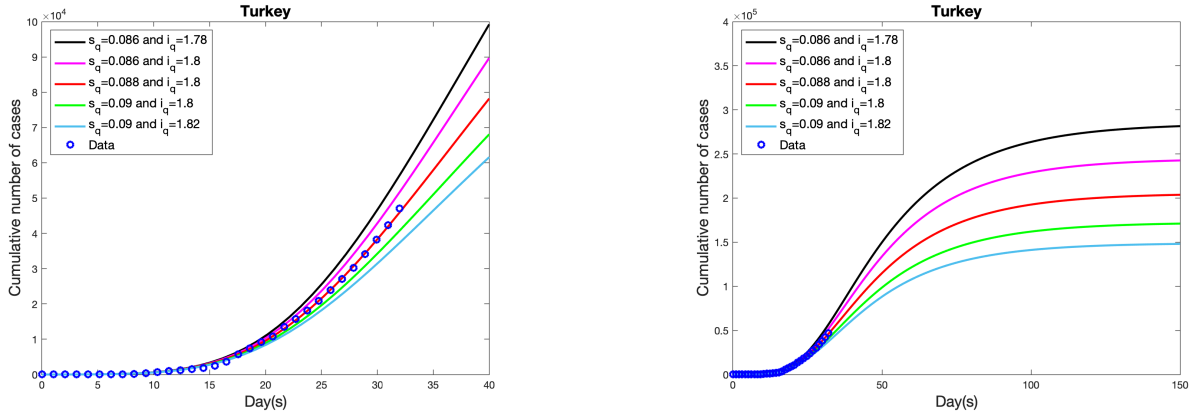

Figure 9: Cumulative number of (infected) cases depending on different quarantine rate s_q and rate of reported cases i_q. The left plot shows the cumulative number of cases between day 1 to day 40, and right plot shows the cumulative number of cases between day 1 to day 150 in the outbreak in Turkey.

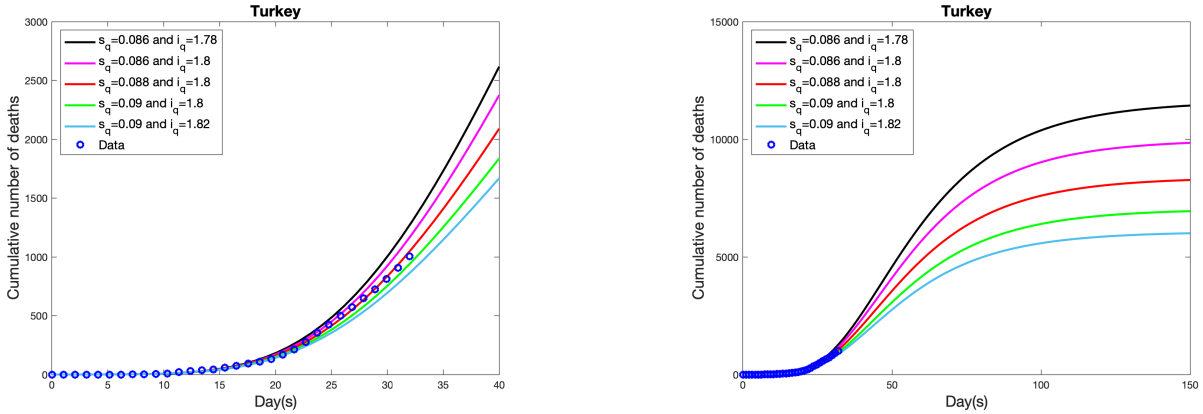

Figure 10: Cumulative number of deaths depending on different quarantine rate s_q and rate of reported cases i_q. The left graph shows the cumulative number of deaths between day 1 to day 40, and right plot shows the cumulative number of deaths between day 1 to day 150 in the outbreak in Turkey.

The peak of the outbreak in Turkey is also very sensitive to the quarantine rate s_q and the rate of reported cases i_q. Depending on the change in quarantine rate and the rate of reported cases i_q, the peak of outbreak in Turkey can be seen between the day 42 (April 20,2020) and day 48 (April 26, 2020), and the outbreak will almost die out by the day 150 (at the end of July 2020, see Figure 11).

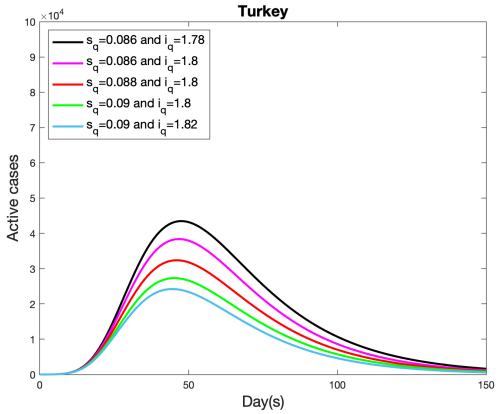

Figure 11: Projected (simulated) peak of outbreak in Turkey depending on different quarantine rate s_q and rate of reported cases, i_q.

7 Conclusion and Discussion

Our analysis suggests that quarantine greatly reduced the number of cases and deaths seen in Hubei's COVID-19 outbreak. In addition, while quarantine does not appear in the representation of $\mathcal{R}_0$, it still indirectly reduces $\mathcal{R}_0$. Our sensitivity analysis indicated that the dynamics of the outbreak are very sensitive to the quarantine rate s_q and contact rate β. The basic reproduction number is estimated as 5.49 and the study shows that any change in β or i_q directly affects the basic reproduction number.

Our study reflected a well-known fact: quarantine decidedly reduces the number of cases and deaths. Increasing (or decreasing) the speed of movement from the susceptible class to the quarantine class by about 10% would double (or half) the number of cases and deaths due to the outbreak (This speed of movement is the rate s_q). Of course, the efficiency of a quarantine (i.e., the level of social distancing) is also very important. In our model, the efficiency of the quarantine is measured by the reduction rate r. The quantity r shows how contact with SARS-CoV-2 decreases due to the quarantine. Naturally, more relaxed quarantine measures allow for a smaller amount of decrease in this contact, while strict quarantine measures radically decrease the amount of contact with the virus which causes COVID-19. As expected, our sensitivity analysis confirmed that this parameter is very important (see Figure 6). Our model shows that the quarantine in Hubei was almost perfect since it caused about 98.9 percent reduction in the contact rate of COVID-19.

Another important parameter that plays a crucial role in the dynamics of the outbreak is the rate of reported cases i_q which is directly related to the number of tests given to detect infected individuals. Similar to the quarantine rate s_q, a 10% reduction (increase) in the rate of reported cases i_q could double (half) the total number of cases/deaths.

As of 30 March 2020, Hubei has reported no new cases for a week prior. At this time, the total number of cases and total number of deaths were 67,801 and 3,187, respectively. Based on our 15-day forecasts, the number of cases in Hubei were projected to be about 67,994 and the number of deaths was projected to be approximately 3,254. Thus, we estimate the fatality rate of the outbreak to be about 4.8% in Hubei. Our model gives about 6% relative error and we are confident that using the model will be helpful for forecasting local outbreaks of the pandemic in other regions.

Based on existing COVID-19 data from Turkey and dynamics learned from the Hubei analysis, the outbreak in Turkey is expected to reach its peak between April 20 and April 26 depending on the number of individuals isolated in quarantine and the number of COVID-19 tests carried out each day in Turkey. The daily number of tests given in Turkey is large when we compare to the rates of reported cases in Hubei. As we showed in the sensitivity analysis, increasing the number of COVID-19 tests and the number of individuals in quarantine will significantly reduce the number of cases (and deaths). Based on our forecasting, the number of cases will be about 203,700 with range 148,100 and 281,500, and the number of deaths will be about 8,269 with range 6,005 and 11,430 depending on quarantine rate, s_q and the rate of

reported cases, i_q in Turkey. Thus, in any cases that are given in Figure 9 and 10, the fatality rate of COVID-19 will be about 4.1% in Turkey.

Based on the results above, our main concern in Turkey is the proportion of people in quarantine. The quarantine rate is 0.088 in Turkey, a low number when we compare with the quarantine rate in Hubei, China (it was 0.096 in Hubei). If Turkey can increase the number of individuals in quarantine, then the number of cases and deaths may decrease significantly (See Figure 9 and 10 to see the effect of quarantine in COVID-19 cases and deaths). Small changes in quarantine rate make significant changes in the total number of cases and deaths in Turkey.

The efficiency of the quarantine in Turkey is about 85 percent, meaning that it causes 85% reduction in the rate of contact with SARS-CoV-2, the virus that causes COVID-19. Thus, the quarantine rate s_q and the efficiency of the quarantine are key factors in the containment of outbreaks and the pandemic as a whole (See Table 3 for reduction rate, r and Figure 6 for the effect of reduction rate in the total number of cases).

Also, the study shows that the rate of reported cases, i_q (related to number of COVID-19 tests) is the most significant parameter in the dynamics of the outbreak after the transmission rate, β (See Table 2). Thus, increasing (decreasing) the number of daily COVID-19 tests can make significant changes in the peak of COVID-19. See Figure 11, increasing the rate of reported cases, i_q shifts the peak of outbreak to earlier dates, and so reduces the total number of cases and deaths in Turkey (See Figures 9 and 10).

As of April 10, 2020, the number of COVID-19 tests given each day in Turkey had increased to 30,000 [14]. If the number is increased further, then it also will decrease the total number of cases and deaths in Turkey (See Figure 9 and 10). Indeed, it is expected that the number of cases may drop below to 203,700 and stay between 148,100 and 203,700. Similarly, this could cause the number of deaths in Turkey to decrease below 8,269 and stay between 6,005 and 8,269.

8 Future Work

Our study leads us to analyze COVID-19 in local perspective regarding the quarantine rate and the rate of reported cases. Therefore, a mathematical model can be developed to quantify the necessary social distance compliance level and the number of tests to be given for each local region as control parameters to eradicate the disease.

In this paper, we developed models for local COVID-19 outbreaks and demonstrated their efficacy toward both high-accuracy forecasting and understanding of dynamics of a local outbreak. The models developed herein can be adapted to accurately model local outbreaks for arbitrary local regions, provided relatively uniform quarantine and testing guidelines are in place and sufficient accurate data are available. The coupling of these models for local regions to obtain reasonable models for larger regions is of great interest and lends novel insight toward the modeling of the COVID-19 pandemic as a whole. Utilizing this approach and the large amount of data available for the United States, the authors will report developments of this nature in a sequel to this work.

Acknowledgements

The authors would like to acknowledge the support of Turkish Ministry of National Education, Batman University, Michigan State University, University of Tennessee at Knoxville in the study.

References

[1] World Health Organization. novel coronavirus (covid-2019) situation reports, 2020. https://www.who.int/emergencies/diseases/novel-coronavirus-2019/situation-reports.

[2] Chinese physicians. ncov.dxy.cn, 2020. https://ncov.dxy.cn/ncovh5/view/pneumonia?scene=2&clicktime=1579582238&enterid=1579582238&from=singlemessage&isappinstalled=0https://ncov.dxy.cn/ncovh5/view/pneumonia?scene=2&clicktime=1579582238&enterid=1579582238&from=singlemessage&isappinstalled=0.

[3] Coronavirus COVID-19 Global Cases by Johns Hopkins CSSE. as, 2020. https://gisanddata.maps.arcgis.com/apps/opsdashboard/index.html#/bda7594740fd40299423467b48e9ecf6.

[4] The New York Times. The coronavirus outbreak, 2020. https://www.nytimes.com/news-event/coronavirus.

[5] Jasper Fuk-Woo Chan, Shuofeng Yuan, Kin-Hang Kok, Kelvin Kai-Wang To, Hin Chu, Jin Yang, Fanfan Xing, Jieling Liu, Cyril Chik-Yan Yip, Rosana Wing-Shan Poon, et al. A familial cluster of pneumonia associated with the 2019 novel coronavirus indicating person-to-person transmission: a study of a family cluster. *The Lancet*, 2020.

[6] Chaolin Huang, Yeming Wang, Xingwang Li, Lili Ren, Jianping Zhao, Yi Hu, Li Zhang, Guohui Fan, Jiuyang Xu, Xiaoying Gu, et al. Clinical features of patients infected with 2019 novel coronavirus in wuhan, china. *The Lancet*, 2020.

[7] Xintian Xu, Ping Chen, Jingfang Wang, Jiannan Feng, Hui Zhou, Xuan Li, Wu Zhong, and Pei Hao. Evolution of the novel coronavirus from the ongoing wuhan outbreak and modeling of its spike protein for risk of human transmission. *Science China Life Sciences*, pages 1–4, 2020.

[8] Natsuko Imai, Ilaria Dorigatti, Anne Cori, Steven Riley, and Neil M Ferguson. Estimating the potential total number of novel coronavirus cases in wuhan city, china, 2020.

[9] Jonathan M Read, Jessica RE Bridgen, Derek AT Cummings, Antonia Ho, and Chris P Jewell. Novel coronavirus 2019-ncov: early estimation of epidemiological parameters and epidemic predictions. *medRxiv*, 2020.

[10] Julien Riou and Christian L Althaus. Pattern of early human-to-human transmission of wuhan 2019-ncov. *bioRxiv*, 2020.

[11] Mingwang Shen, Zhihang Peng, Yanni Xiao, and Lei Zhang. Modelling the epidemic trend of the 2019 novel coronavirus outbreak in china. *bioRxiv*, 2020.

[12] Shi Zhao, Qianyin Lin, Jinjun Ran, Salihu S Musa, Guangpu Yang, Weiming Wang, Yijun Lou, Daozhou Gao, Lin Yang, Daihai He, et al. Preliminary estimation of the basic reproduction number of novel coronavirus (2019-ncov) in china, from 2019 to 2020: A data-driven analysis in the early phase of the outbreak. *International Journal of Infectious Diseases*, 2020.

[13] Zhidong Cao, Qingpeng Zhang, Xin Lu, Dirk Pfeiffer, Zhongwei Jia, Hongbing Song, and Daniel Dajun Zeng. Estimating the effective reproduction number of the 2019-ncov in china. *medRxiv*, 2020.

[14] Ministry of Health (Turkey). Coronavirus disease 2019 (covid-19) daily data, 2020. https://covid19.saglik.gov.tr.

[15] Mikayla Chubb and Kathryn Jacobsen. Mathematical modeling and the epidemiological research process. *European Journal of Epidemiology*, 25(1):13–19, 2010.

[16] M. J. Keeling and P Rohani. Modeling infectious diseases in humans and animals. *Biometrics*, 64(3):993–993, 2008.

[17] Mark Kot. *Elements of mathematical ecology*. Cambridge University Press, Cambridge ; New York, NY, 2001.

[18] Hiroshi Nishiura, Natalie M Linton, and Andrei R Akhmetzhanov. Serial interval of novel coronavirus (2019-ncov) infections. *medRxiv*, 2020.

[19] Wei-jie Guan, Zheng-yi Ni, Yu Hu, Wen-hua Liang, Chun-quan Ou, Jian-xing He, Lei Liu, Hong Shan, Chun-liang Lei, David SC Hui, et al. Clinical characteristics of 2019 novel coronavirus infection in china. *MedRxiv*, 2020.

[20] Steven Sanche, Yen Ting Lin, Chonggang Xu, Ethan Romero-Severson, Nicolas W Hengartner, and Ruian Ke. The novel coronavirus, 2019-ncov, is highly contagious and more infectious than initially estimated. *arXiv preprint arXiv:2002.03268*, 2020.

[21] World Health Organization. Crude birth and death rate data by country, 2020. http://apps.who.int/gho/data/node.main.CBDR107?lang=en.

[22] Odo Diekmann, JAP Heesterbeek, and Michael G Roberts. The construction of next-generation matrices for compartmental epidemic models. *Journal of the Royal Society Interface*, 7(47):873–885, 2010.

[23] Pauline Van den Driessche and James Watmough. Reproduction numbers and sub-threshold endemic equilibria for compartmental models of disease transmission. *Mathematical biosciences*, 180(1-2):29–48, 2002.

[24] P Van den Driessche and James Watmough. *Further notes on the basic reproduction number*. Springer, 2008.

[25] Simeone Marino, Ian B. Hogue, Christian J. Ray, and Denise E. Kirschner. A methodology for performing global uncertainty and sensitivity analysis in systems biology. *Journal of Theoretical Biology*, 254(1):178–196, 2008.